

Evading Anderson localization in a one-dimensional conductor with correlated disorder

Onuttom Narayan

Physics Department, University of California, Santa Cruz, California 95064, USA

Harsh Mathur

*Department of Physics, Case Western Reserve University, Cleveland, Ohio 44106-7079, USA*Richard Montgomery *Mathematics Department, University of California, Santa Cruz, California 95064, USA*

(Received 2 November 2020; accepted 6 April 2021; published 21 April 2021)

We show that a one-dimensional disordered conductor with correlated disorder has an extended state and a Landauer resistance that is nonzero in the limit of infinite system size in contrast to the predictions of the scaling theory of Anderson localization. The delocalization transition is not related to any underlying symmetry of the model such as particle-hole symmetry. Moreover, the form of correlated disorder considered here is distinct from other models with delocalization transitions that have been considered in the literature. For a wire of finite length the effect manifests as a sharp transmission resonance that narrows as the length of the wire is increased. Experimental realizations and applications are discussed including the possibility of constructing a narrow-band light filter.

DOI: [10.1103/PhysRevB.103.144203](https://doi.org/10.1103/PhysRevB.103.144203)**I. INTRODUCTION**

In a seminal paper in 1958, Anderson demonstrated that in disordered solids electronic states may be localized over a range of energies [1]. Over the next two decades, it was established that in one and two dimensions electronic states are always localized, no matter how weak the disorder, while in three dimensions localized and extended states can exist over different ranges of energy, separated by a mobility edge [2]. These findings completely subverted the simple dogma of band theory by showing that, for weakly interacting electrons, disorder—rather than the band structure in the clean limit—determined whether a material is a conductor or insulator at low temperature [3]. Moreover, Anderson localization proved relevant to optics, acoustics, cold atoms, neural networks, medical imaging, and in general to any problem of coherent propagation of waves in a random medium [4]. Here, we show that, contrary to this well-established paradigm, a one-dimensional disordered conductor with correlated disorder may have an extended state and a Landauer resistance that is nonzero in the infinite size limit. The delocalization transition is unrelated to any underlying symmetry of the model such as particle-hole symmetry. For a wire of finite length the effect manifests as a sharp transmission resonance that narrows as the length of the wire is increased. Experimental realizations may be possible using metamaterials and might find application as fault-tolerant narrow-band light filters.

Anderson localization is particularly well established in one dimension where it is possible to derive exact results and even rigorous proofs of localization for appropriate models [5,6]. Two distinct approaches have been developed to describe the universal features of localization. The first

approach, grounded in random matrix theory, posits that the distribution of transfer matrices in one dimension undergoes diffusion in the space of possible transfer matrices as a function of the length of the conductor [7]. This approach, which is restricted to one dimension, reveals that the conductance has a broad log normal distribution, with very different typical and mean values, both of which decay exponentially with the length of the system (a highly non-Ohmic size dependence). Field theory methods, based on replicas [8] or supersymmetry [9] for disorder averaging, likewise describe the universal features of localization on length scales that are large compared to the microscopic elastic scattering length, and confirm the picture described above.

One known exception to complete localization in one dimension is systems with particle-hole symmetry [10]. In this case at the symmetric point of zero energy there is an extended state and hence a delocalization transition that separates Anderson insulators above and below zero energy. More generally, the discovery that quantum systems can be classified into ten symmetry classes [11] based on the absence or presence of particle-hole and time-reversal symmetries has furnished additional examples of delocalization at zero energy [12]. Another example of an extended state at an isolated energy is provided by the quantum dimer model [13]. In this case the delocalization happens because the individual scatterers become transparent at a common resonant energy, making the system effectively clean at that energy. A third exceptional circumstance that has been identified in the literature is the case of disorder with long-range spatial correlations. In this case it is found that there can be a band of extended states separated from the localized states by a mobility edge [14–17].

In the same vein as the papers noted above here we report a model that undergoes a delocalization transition. Our model does not possess any underlying symmetries or depend on the transparency of individual impurities. It has correlated disorder but of a form distinct from previous models considered in the literature [14–17]. Our model consists of symmetric scatterers that are separated by variable distances. Both the strength of the individual scatterers and the spacing between them are random variables. However, there are correlations among these random variables: The strengths of the scatterers are independent random variables but the spacing between the successive scatterers is constrained by the strengths of the scatterers. Respecting these constraints leads inexorably to an extended state. As discussed below it may be possible to fabricate single-mode waveguides with this type of disorder.

The remainder of the paper is organized as follows. In Sec. II we introduce the model and show that it can be obtained from an underlying tight-binding model with on-site disorder. In Sec. III we demonstrate using a combination of analytic arguments and numerical simulations that the probability of nonzero conductance remains finite no matter how long the conductor grows, contrary to the localization paradigm. In Sec. IV we offer some concluding remarks on possible experimental tests, applications, and open questions.

II. THE MODEL

A. Individual scatterers

To be concrete, we consider Anderson’s model of a one-dimensional lattice with noninteracting electrons and nearest-neighbor hopping. The corresponding Schrödinger equation is the difference equation

$$\psi_{n-1} + V_n \psi_n + \psi_{n+1} = E \psi_n. \quad (1)$$

Here, ψ_n is the wave function at site n and V_n is the site potential which is either zero or a random number between $-W$ and W . Note that in the absence of disorder ($V_n = 0$ for all n) the solutions are plane waves $\psi_n = \exp(ikn)$ with energy $E = 2 \cos k$. Sites where $V_n \neq 0$ are called scatterers, and we constrain the system so that two scatterers cannot be adjacent to each other. Thus the system can be understood as a sequence of scatterers separated by free propagation segments of variable length. Our strategy will be to find the S matrix for each scatterer and combine them iteratively to obtain the S matrix for the entire system.

First, let us consider the S matrix for a single impurity in the tight-binding model located at the position $n = 0$ (Fig. 1). We make the ansatz

$$\begin{aligned} \psi_n &= a_L \exp(ikn) + a'_L \exp(-ikn) \quad \text{for } n \leq 0 \\ &= a_R \exp(ikn) + a'_R \exp(-ikn) \quad \text{for } n \geq 0. \end{aligned} \quad (2)$$

Making use of the Schrödinger Eq. (1) for $n = 0$ we obtain

$$\begin{aligned} a_L + a'_L &= \psi, \\ a_R + a'_R &= \psi, \\ (2 \cos k - V) \psi &= a_L e^{-ik} + a'_L e^{ik} + a_R e^{ik} + a'_R e^{-ik}. \end{aligned} \quad (3)$$

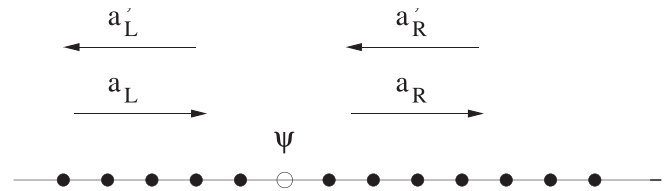


FIG. 1. A scattering site, with incoming and outgoing waves on both sides. The wave function at the scattering site is ψ . The phases of the waves on both sides are chosen so that the amplitude would have been $a_{L,R} + a'_{L,R}$ at the scattering site if the waves from the left/right were to continue uninterrupted through the scattering site.

Solving Eq. (3) yields

$$\begin{pmatrix} a'_L \\ a_R \end{pmatrix} = S \begin{pmatrix} a_L \\ a'_R \end{pmatrix}. \quad (4)$$

Here, the 2×2 S matrix that connects the outgoing amplitudes to the incoming amplitudes is given by

$$S(V, k) = -\frac{1}{2i \sin k + V} \begin{pmatrix} V & -2i \sin k \\ -2i \sin k & V \end{pmatrix}. \quad (5)$$

The form of the S matrix for a single scatterer is powerfully constrained by general principles. Probability conservation imposes unitarity, $S^\dagger S = 1$. Parity imposes the additional requirements that $S_{11} = S_{22}$ and $S_{12} = S_{21}$. The most general 2×2 matrix consistent with these requirements may be parametrized as

$$S = e^{i\gamma} \begin{pmatrix} \cos \theta & i \sin \theta \\ i \sin \theta & \cos \theta \end{pmatrix}, \quad (6)$$

where $0 \leq \theta \leq \pi/2$ and $0 \leq \gamma < 2\pi$. It follows from Eqs. (4) and (6) that the transmission coefficient is $\sin^2 \theta$ and the reflection coefficient is $\cos^2 \theta$. Here, we refer to the parameter θ as the opacity of the S matrix.

A comparison of Eqs. (5) and (6) shows that for the tight-binding model analyzed above, the opacity θ and the overall phase γ for a single scatterer are given by

$$\begin{aligned} \exp(i\theta) &= \pm \frac{V - 2i \sin k}{\sqrt{V^2 + 4 \sin^2 k}}, \\ \exp(i\gamma) &= \mp \frac{\sqrt{V^2 + 4 \sin^2 k}}{V + 2i \sin k} = -\exp(i\theta), \end{aligned} \quad (7)$$

where the sign on the right-hand side is positive (negative) when V is positive (negative), i.e., $\cos \theta > 0$. The fact that θ and γ are related for this model is not true in general. This coincidence will play no role in our subsequent analysis.

B. Combining scatterers

The complete lattice can be treated as a sequence of scatterers, separated by free propagation segments of variable length. Since the lattice is not left-right symmetric, the S matrix of the entire system is not as constrained as Eq. (6). Nevertheless, time-reversal invariance requires that $S^* = S^{-1}$ which, together with the unitarity of S , implies that $S = S^T$.

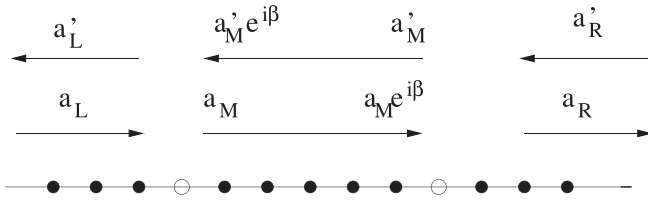


FIG. 2. Two scatterers, with waves propagating to the left and to the right in each region. In the middle region, the left-moving wave is incoming for the first scatterer and outgoing for the second scatterer, and vice versa for the right-moving wave. The phases of both of these are defined to be zero at the scatterer they start from, and $\exp[ik(L+1)] = \exp[i\beta]$ at the scatterer they end up at, where k is the wave vector and L is the length of the region between the scatterers; in the figure, $L = 5$.

Therefore we obtain the parametrization

$$S_N = e^{i\gamma_N} \begin{pmatrix} \cos \theta_N e^{i\delta_N} & i \sin \theta_N \\ i \sin \theta_N & \cos \theta_N e^{-i\delta_N} \end{pmatrix}, \quad (8)$$

where S_N is the S matrix of a lattice with N scatterers and the parameters lie in the domain $0 \leq \theta_N \leq \pi/2$, $0 \leq \delta_N < 2\pi$, and $0 \leq \gamma_N < 2\pi$.

Now suppose that a lattice with N scatterers has an additional impurity attached to its end with L sites between the N th and $(N+1)$ th scatterer. The amplitudes of the waves in the different regions are as shown in Fig. 2. In the intermediate region the forward and backward waves have amplitudes a_M and a'_M , respectively. The phases are chosen so that at the site immediately to the right of the N th scatterer the wave function is $a_M \exp(ik) + a'_M \exp(ikL)$. Hence at the site immediately to the left of the $(N+1)$ th scatterer the wave function is $a_M \exp(ikL) + a'_M \exp(ik)$. Defining $\exp(i\beta) = \exp[ik(L+1)]$ we have

$$\begin{pmatrix} a'_M \\ a_R \end{pmatrix} = S \begin{pmatrix} a_M e^{i\beta} \\ a'_R \end{pmatrix}, \quad (9)$$

where S is the S matrix of the $(N+1)$ th impurity. On the other hand, the effect of the N previous scatterers can be represented as

$$\begin{pmatrix} a'_L \\ a_M \end{pmatrix} = S_N \begin{pmatrix} a_L \\ a'_M e^{i\beta} \end{pmatrix}. \quad (10)$$

Our objective is to calculate S_{N+1} , the S matrix for the combined system, which is defined by

$$\begin{pmatrix} a'_L \\ a_R \end{pmatrix} = S_{N+1} \begin{pmatrix} a_L \\ a'_R \end{pmatrix}. \quad (11)$$

By eliminating the intermediate amplitudes from Eqs. (9) and (10), after a lengthy but straightforward calculation, we obtain

$$\begin{aligned} \cos \theta_{N+1} e^{i(\gamma_{N+1} + \delta_{N+1})} &= e^{i(\gamma_N + \delta_N)} \frac{\cos \theta_N - \cos \theta e^{i\phi}}{1 - \cos \theta \cos \theta_N e^{i\phi}}, \\ \cos \theta_{N+1} e^{i(\gamma_{N+1} - \delta_{N+1})} &= e^{i\gamma} \frac{\cos \theta - \cos \theta_N e^{i\phi}}{1 - \cos \theta \cos \theta_N e^{i\phi}}, \\ i \sin \theta_{N+1} e^{i\gamma_{N+1}} &= -e^{i(\gamma + \gamma_N + \delta_N)/2} \frac{\sin \theta \sin \theta_N e^{i\phi/2}}{1 - \cos \theta \cos \theta_N e^{i\phi}}. \end{aligned} \quad (12)$$

Here, we have defined $\phi = 2\beta + \gamma + \gamma_N - \delta_N$. Note that ϕ depends on the phases of the two S matrices being combined and through β also on the distance between the new $(N+1)$ th scatterer and its predecessor.

Equation (12) is the main result of this section. It relates the parameters of the $N+1$ scatterer S matrix, $(\theta_{N+1}, \gamma_{N+1}, \delta_{N+1})$, to $(\theta_N, \gamma_N, \delta_N)$ and (θ, γ) , the parameters of the S matrices for the first N scatterers and for the $(N+1)$ th scatterer, respectively.

Although we have couched our discussion in terms of a tight-binding Anderson model it should be obvious that our analysis is much more general. For example, it also applies to a continuum model in which the scatterers are rectangular top-hat potentials of variable heights and widths separated by variable distances. The only difference is that now the opacity and phase of the S matrix would be determined by the barrier height and width of the scatterer.

III. DELOCALIZATION

A. Analytical results

Now suppose that a lattice with N scatterers has an additional scatterer attached to its end. The S matrix of the composite system, S_{N+1} , can be obtained by composing S_N and S , the S matrices of the component parts as shown above. Here, we focus on the transmission coefficient which, according to Landauer's formula [18], is the conductance of the system in units of e^2/h . It follows from Eq. (12) that the transmission coefficient evolves according to

$$\sin^2 \theta_{N+1} = \frac{\sin^2 \theta \sin^2 \theta_N}{1 + \cos^2 \theta \cos^2 \theta_N - 2 \cos \theta \cos \theta_N \cos \phi}. \quad (13)$$

Here, recall that we have defined $\phi = 2\beta + \gamma + \gamma_N - \delta_N$. Note that ϕ depends on the phases of the two S matrices being combined and, through β , also on the distance between the new $(N+1)$ th scatterer and its predecessor. Specifically, $\beta = k(L+1)$ for the lattice model where L is the number of lattice sites between the N th scatterer and the $(N+1)$ th. In the continuum limit $\beta = kL$, where L is the distance between successive scatterers. Similar relations can be written down that give the phases γ_{N+1} and δ_{N+1} in terms of the parameters of the matrices S_N and S , but for the sake of brevity they are omitted. We now describe how Eq. (13) conventionally leads to Anderson localization and how correlated disorder may evade it.

If the scatterers are dilute and randomly distributed then ϕ can be treated as a uniform random variable. Making this assumption and averaging the reciprocal of Eq. (13) over the parameters of all the scatterers we obtain

$$\langle \csc^2 \theta_{N+1} \rangle = [1 + 2\langle \cot^2 \theta \rangle] \langle \csc^2 \theta_N \rangle - \langle \cot^2 \theta \rangle. \quad (14)$$

To obtain this result we take into account that the opacity and phase of the $(N+1)$ th scatterer are independent of those that preceded it. The only assumption we have to make about the distribution of (θ, γ) is that the probability of opaque scatterers is small (more precisely, we assume that the probability of small opacity θ goes to zero sufficiently fast that $\langle \cot^2 \theta \rangle$ is finite). This is certainly the case for the Anderson tight-binding model and for any other reasonable model we

might consider. By iterating Eq. (14) it is easy to see that $\langle \text{csc}^2 \theta_N \rangle$, which has the interpretation of the mean resistance of the sample, grows exponentially with the system size N . This is the essence of Anderson localization. Note our analysis only shows that the mean resistance grows exponentially but for the Anderson model it is in fact possible to derive the full distribution of resistance [19].

Now let us look for a qualitatively different fixed point for the evolution Eq. (13). To this end at first we assume that all the scatterers are identical and have the same opacity θ . We also assume that the phase ϕ can be held constant for each successive scatterer that is added to the system. With these assumptions Eq. (13) is a simple deterministic map for θ_N with a fixed point θ^* given by

$$1 = \frac{\sin^2 \theta}{1 + \cos^2 \theta \cos^2 \theta_* - 2 \cos \theta \cos \theta_* \cos \phi}. \quad (15)$$

As long as $\cos \phi / \cos \theta > 1$, or equivalently $-\theta < \phi < \theta$, this equation has a solution. The condition for θ_* to be a stable fixed point is $-1 < d \sin^2 \theta_{N+1} / d \sin^2 \theta_N < 1$ at $\theta_N = \theta_{N+1} = \theta_*$ and can be verified to be always satisfied.

Now let us return to the disordered problem. In this case the opacity θ is drawn from a distribution each time Eq. (13) is evolved. To try to retain the nontrivial solution for the deterministic case found above we constrain ϕ to be a random variable drawn from a distribution that satisfies the solvability condition $-\theta < \phi < \theta$ noted above. Note that if we imagine building the system one scatterer at a time what we are effectively saying is that the position of the $(N+1)$ th scatterer is constrained to lie within a certain interval that is determined by the S matrix of the preceding N scatterers. However, within that range we can place the $(N+1)$ th scatterer at random. Hence the system we are considering is random but with correlated disorder. We now show that this random system evades Anderson localization.

To this end we again take the reciprocal of both sides of Eq. (13) and average over disorder to obtain

$$\langle \text{csc}^2 \theta_{N+1} \rangle = \langle \text{csc}^2 \theta_N \rangle \langle \text{csc}^2 \theta \rangle + \langle \cot^2 \theta_N \rangle \langle \cot^2 \theta \rangle - 2 \langle \cot \theta_N \text{csc} \theta_N \rangle \langle \cot \theta \text{csc} \theta \cos \phi \rangle. \quad (16)$$

We have used the fact that θ is independent of θ_N and ϕ is correlated with θ , not with θ_N . For simplicity let us assume that ϕ is uniformly distributed over the interval $-\theta$ to θ . Performing the average of ϕ we then obtain

$$\langle \text{csc}^2 \theta_{N+1} \rangle = \langle \text{csc}^2 \theta_N \rangle \langle \text{csc}^2 \theta \rangle + \langle \cot^2 \theta_N \rangle \langle \cot^2 \theta \rangle - 2 \langle \cot \theta_N \text{csc} \theta_N \rangle \langle \cot \theta / \theta \rangle. \quad (17)$$

With some rearrangement Eq. (17) can be brought to the form

$$\langle \text{csc}^2 \theta_{N+1} \rangle - \langle \text{csc}^2 \theta_N \rangle = -2B \langle \text{csc}^2 \theta_N \rangle + C_N. \quad (18)$$

Here, B is given by

$$B = \left\langle \frac{\cot \theta}{\theta} - \cot^2 \theta \right\rangle = \left\langle \cot^2 \theta \left(\frac{\tan \theta}{\theta} - 1 \right) \right\rangle \quad (19)$$

and is evidently a finite positive constant since $\tan \theta \geq \theta$ over the interval from zero to $\pi/2$. The specific value of B will depend on the distribution chosen for the opacity θ . The

quantity denoted C_N in Eq. (18) is given by

$$C_N = \left[\left\langle \frac{\cot \theta}{\theta} \right\rangle \langle R(\theta_N) \rangle - \langle \cot^2 \theta \rangle \right]. \quad (20)$$

Here, $R(\theta_N) = 2(1 - \cos \theta_N) / \sin^2 \theta_N$ is a monotonic decreasing function that goes from 1 to zero as θ_N goes from zero to $\pi/2$. Hence C_N is finite and lies in the range between $-\langle \cot^2 \theta \rangle$ and B .

Equation (18) precludes Anderson localization. For a localized conductor the average resistance should grow monotonically and without bound. However, if $\langle \text{csc}^2 \theta_N \rangle$ gets sufficiently large, then the right-hand side of Eq. (18) becomes negative, contradicting the assumption that $\langle \text{csc}^2 \theta_N \rangle$ was growing monotonically without bound. Rather, if the mean resistance is growing monotonically, Eq. (18) shows that it must saturate to a value less than unity (in units of h/e^2). Even if we relax the assumption of monotonic behavior, Eq. (18) shows that the resistance is bounded, which is incompatible with Anderson localization. Moreover, the finiteness of $\langle \text{csc}^2 \theta_N \rangle$ shows that the distribution $P(\theta_N)$ must vanish as $\theta_N \rightarrow 0$.

B. Numerical results

To test these predictions we have numerically simulated an Anderson model with correlated disorder of the type described above. In our simulations each scatterer has an S matrix of the form of Eq. (5) with V chosen uniformly over the interval $-W < V < W$ with $W = 0.3$ and the energy is given by $2 \sin k = 1.6$. For these values of k and W the distribution of θ is narrow with support close to $\theta = \pi/2$. N scatterers are then combined one by one with the angle ϕ drawn in each instance from a uniform distribution over the range

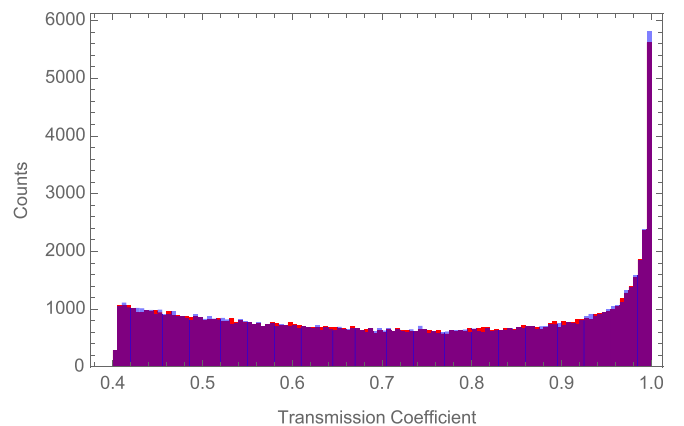


FIG. 3. Histogram of $\sin^2 \theta_N$. Each scatterer has the potential V chosen at random, uniformly over the interval $[-0.3, 0.3]$. The angle θ associated with a scatterer is $\cos^{-1}(|V|/\sqrt{V^2 + 4 \sin^2 k})$, where we have chosen the energy $2 \cos k$ to be 1.2. The phase ϕ between each scatterer and its predecessor is chosen to be a uniform random variable over the interval $0 < \phi < \theta$. The histogram is plotted for 10^5 random lattices with $N = 100$ scatterers (blue) and $N = 10000$ scatterers (red). No significant difference is seen between the two. Note that the distribution drops to zero below a transmission coefficient of approximately 0.4. The existence of a lower cutoff for the distribution can be shown analytically.

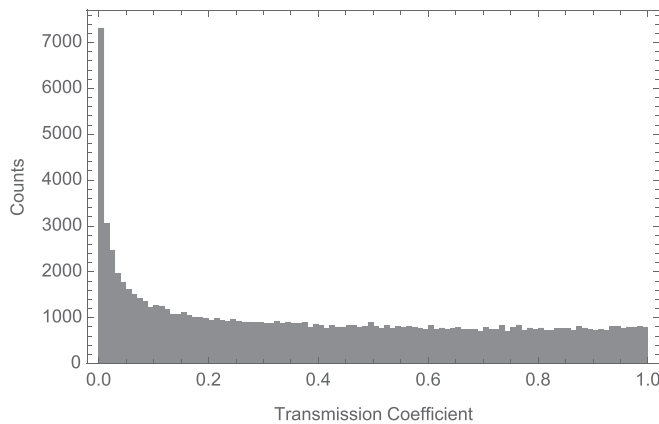


FIG. 4. Histogram of $\sin^2 \theta_N$. The angle θ for each scatterer is chosen to be a uniform random variable in the first quadrant, and the angle ϕ is a uniform random variable between 0 and θ . The histogram is constructed from 10^5 lattices with $N = 1000$; increasing N does not change this significantly. Although there is a peak in the histogram at $\sin^2 \theta_N = 0$, possibly a divergence, there is a long tail to the distribution, and $\langle \sin^2 \theta_\infty \rangle$ is nonzero.

$-\theta < \phi < \theta$. We calculate the transmission $\sin^2 \theta_N$ for $M = 10^5$ distinct realizations and histogram the M distinct values of the dimensional conductance (Fig. 3). Histograms for $N = 100$ and $N = 10\,000$ show no significant difference showing that the $N \rightarrow \infty$ limit has been reached.

Figure 3 shows the distribution of the conductance reaches a steady state as the length of the conductor is increased and, moreover, that the mean conductance remains finite in the limit $N \rightarrow \infty$, consistent with our analytic arguments. By contrast, if we do not constrain the distribution of ϕ , we obtain the very different behavior characteristic of a localized system, namely that the distribution is peaked near zero transmission and it does not saturate but rather the mean and typical value continue to diminish rapidly with N . We have also performed simulations taking θ to be uniformly distributed over the interval from zero to $\pi/2$. In this case also we find delocalization (see Fig. 4) even though a uniformly distributed opacity violates the assumption made in our analytic argument

that $(\cot^2 \theta)$ is finite. This is logically possible because the conditions of our argument are sufficiently not necessary and it demonstrates the robustness of delocalization in the presence of correlated disorder.

We should draw attention to the fact that in order to obtain delocalization we had to build up our disordered conductor by choosing the phase ϕ for each successive scatterer to lie in an appropriate range of positions. The appropriate range depends on the energy parameter k , so the question arises whether the conductor will remain delocalized if the energy is varied. Our simulations show that the phase ϕ is extremely sensitive to the energy parameter k and fails to satisfy the constraint that $-\theta < \phi < \theta$ as the energy is varied. Hence the delocalized state is an isolated state. For a finite system it manifests as a transmission resonance that narrows as $N \rightarrow \infty$.

IV. CONCLUSION

We have described a one-dimensional conductor that undergoes a delocalization transition. The transition is not related to any symmetry of the problem or traceable to the effective transparency of the individual scatterers. The model has correlated disorder but distinct from the forms previously considered in the literature (see, e.g., Refs. [14–17]). Conceptually the delocalized structure is constructed scatterer by scatterer so it is natural to expect that it can be most readily realized experimentally as a stacking of films much as a one-dimensional photonic crystal [20]. A possible application of such a structure is as an extremely narrow-band filter for light. In contrast to a photonic crystal the structure does not have to be engineered with precision; the randomness is in fact essential to the operation of the filter. Cold atoms are another experimental arena for localization studies wherein correlated disorder may be realizable [21]. An interesting analog of Anderson localization is provided by the phenomenon of dynamical localization in kicked quantum rotors [22]. Another closely related problem is that of localization in quasirandom systems where it has been demonstrated that long-range correlations also lead to delocalization [23–26]. Whether the ideas discussed in this paper can be exported to that context or generalized to two and higher dimensions are interesting open questions.

-
- [1] P. W. Anderson, Absence of diffusion in certain random lattices, *Phys. Rev.* **109**, 1492 (1958).
 - [2] E. Abrahams, P. W. Anderson, D. C. Licciardello, and T. V. Ramakrishnan, Scaling Theory of Localization: Absence of Quantum Diffusion in Two Dimensions, *Phys. Rev. Lett.* **42**, 673 (1979).
 - [3] P. A. Lee and T. V. Ramakrishnan, Disordered electronic systems, *Rev. Mod. Phys.* **57**, 287 (1985).
 - [4] For an entry point into the vast literature, see, for example, A. Lagendijk, B. van Tiggelen, and D. Wiersma, Fifty years of Anderson localization, *Phys. Today* **62(8)**, 24 (2009); *50 Years of Anderson Localization*, edited by E. Abrahams (World Scientific, Singapore, 2010).
 - [5] K. Ishii, Localization of eigenstates and transport phenomena in 1D disordered systems, *Prog. Theor. Phys. Suppl.* **53**, 77 (1971).
 - [6] P. W. Anderson, D. J. Thouless, E. Abrahams, and D. S. Fisher, New method for a scaling theory of localization, *Phys. Rev. B* **22**, 3519 (1980).
 - [7] C. W. J. Beenakker, Random matrix theory of quantum transport, *Rev. Mod. Phys.* **69**, 731 (1997).
 - [8] A. J. McKane and M. Stone, Localization as an alternative to Goldstone's theorem, *Ann. Phys.* **131**, 36 (1981).
 - [9] K. B. Efetov, *Supersymmetry in Disorder and Chaos* (Cambridge University Press, Cambridge, U.K., 1996).
 - [10] L. Balents and M. P. A. Fisher, Delocalization transition via supersymmetry in one dimension, *Phys. Rev. B* **56**, 12970 (1997);

- H. Mathur, Feynman's propagator applied to network models of localization, *ibid.* **56**, 15794 (1997).
- [11] A. Altland and M. R. Zirnbauer, Nonstandard symmetry classes in mesoscopic normal superconducting hybrid structures, *Phys. Rev. B* **55**, 1142 (1997).
- [12] P. W. Brouwer, A. Furusaki, I. A. Gruzberg, and C. Mudry, Localization and Delocalization in Dirty Superconducting Wires, *Phys. Rev. Lett.* **85**, 1064 (2000); O. Motrunich, K. Damle, and D. A. Huse, Griffiths effects and quantum critical points in dirty superconductors without spin-rotation invariance: One-dimensional examples, *Phys. Rev. B* **63**, 224204 (2001); I. A. Gruzberg, N. Read, and S. Vishveshwara, Localization in disordered superconducting wires with broken spin-rotation symmetry, *ibid.* **71**, 245124 (2005).
- [13] D. H. Dunlap, H.-L. Wu, and P. W. Phillips, Absence of Localization in a Random Dimer Model, *Phys. Rev. Lett.* **65**, 88 (1990).
- [14] F. A. B. F. de Moura and M. L. Lyra, Delocalization in the 1D Anderson Model with Long-Range Correlated Disorder, *Phys. Rev. Lett.* **81**, 3735 (1998).
- [15] T. Kaya, Localization-delocalization transition in chains with long-range correlated disorder, *Eur. Phys. J. B* **55**, 49 (2007).
- [16] M. O. Sales and F. A. B. F. de Moura, Numerical study of the one-electron dynamics in one-dimensional systems with short-range correlated disorder, *Physica E* **45**, 97 (2012).
- [17] G. M. Petersen and N. Sandler, Anticorrelations from power-law spectral disorder and conditions for an Anderson transition, *Phys. Rev. B* **87**, 195443 (2013).
- [18] H. U. Baranger and A. D. Stone, Electrical linear-response theory in an arbitrary magnetic field: A new Fermi-surface formulation, *Phys. Rev. B* **40**, 8169 (1989).
- [19] P. D. Kirkman and J. B. Pendry, The statistics of one-dimensional resistances, *J. Phys. C* **17**, 4327 (1984).
- [20] J. D. Joannopoulos, S. G. Johnson, J. N. Winn, and R. D. Meade, *Photonic Crystals: Molding the Flow of Light*, 2nd ed. (Princeton University Press, Princeton, NJ, 2008).
- [21] S. S. Kondov, W. R. McGehee, J. J. Zirbel, and B. DeMarco, Three-dimensional Anderson localization of ultracold matter, *Science* **334**, 66 (2011); F. Jendrzejewski, A. Bernard, K. Muller, P. Cheinet, V. Josse, M. Piraud, L. Pezze, L. Sanchez-Palencia, A. Aspect, and P. Bouyer, Three-dimensional localization of ultracold atoms in an optical disordered potential, *Nat. Phys.* **8**, 398 (2012); G. Semeghini, M. Landini, P. Castilho, S. Roy, G. Spagnolli, A. Trenkwalder, M. Fattori, M. Inguscio, and G. Modugno, Measurement of the mobility edge for 3D Anderson localization, *ibid.* **11**, 554 (2015).
- [22] D. R. Grempel, R. E. Prange, and S. Fishman, Quantum dynamics of a nonintegrable system, *Phys. Rev. A* **29**, 1639 (1984); F. L. Moore, J. C. Robinson, C. Bharucha, P. E. Williams, and M. G. Raizen, Observation of Dynamical Localization in Atomic Momentum Transfer: A New Testing Ground for Quantum Chaos, *Phys. Rev. Lett.* **73**, 2974 (1994).
- [23] H. Hiramoto and M. Kohmoto, Scaling analysis of quasiperiodic systems: Generalized Harper model, *Phys. Rev. B* **40**, 8225 (1989).
- [24] D. J. Boers, B. Goedeke, D. Hinrichs, and M. Holthaus, Mobility edges in bichromatic optical lattices, *Phys. Rev. A* **75**, 063404 (2007).
- [25] C. Danieli, K. Rayanov, B. Pavlov, G. Martin, and S. Flach, Approximating metal insulator transitions, *Int. J. Mod. Phys. B* **29**, 1550036 (2015).
- [26] S. Ganeshan, J. H. Pixley, and S. Das Sarma, Nearest Neighbor Tight Binding Models with an Exact Mobility Edge in One Dimension, *Phys. Rev. Lett.* **114**, 146601 (2015).